

Multicomponent wide band gap oxide semiconductors for thin film transistors

E. Fortunato, P. Barquinha, L. Pereira, G. Gonçalves, R. Martins

Materials Science Department/CENIMAT, FCT-UNL, Campus da Caparica, Portugal

Phone: +351 212 948 562, E-mail: elvira.fortunato@fct.unl.pt

Abstract

The recent application of wide band gap oxide semiconductors to transparent thin film transistors (TTFTs) is making a fast and growing (r)evolution on the contemporary solid-state electronics. In this paper we present some of the recent results we have obtained using wide band gap oxide semiconductors, like indium zinc oxide, produced by rf sputtering at room temperature. The devices work in the enhancement mode and exhibit excellent saturation drain currents. On-off ratios above 10^6 are achieved. The optical transmittance data in the visible range reveals average transmittance higher than 80 %, including the glass substrate. Channel mobilities are also quite respectable, with some devices presenting values around $25 \text{ cm}^2/\text{Vs}$, even without any annealing or other post deposition improvement processes. The high performances presented by these TTFTs associated to a high electron mobility, at least two orders of magnitude higher than that of conventional amorphous silicon TFTs and a low threshold voltage, opens new doors for applications in flexible, wearable, disposable portable electronics as well as battery-powered applications.

1. Introduction

Since 2003 several reports on fully transparent TFTs have been presented. Despite the semiconductor material used in the first devices was, in most cases, zinc oxide [1-4], more recently some groups have presented transistors based on multicomponent amorphous oxides, mainly due to the high electron mobilities of these materials, despite their amorphous structure [5-7]. Some examples of the multicomponent oxides used on TTFTs are indium gallium zinc oxide [5], zinc tin oxide [6] and zinc indium oxide [7], which allowed already to produce devices with field effect mobilities reaching $50 \text{ cm}^2/\text{Vs}$ [7], on-off ratios of $\sim 10^7$ [6] and even flexible transistors [5]. Indium zinc oxide (IZO) is another potential

candidate for the active layer of TTFTs, exhibiting an optical transmittance in the visible region greater than 84 %, an optical band-gap around 3.7 eV, mobility exceeding $60 \text{ cm}^2/\text{Vs}$ and resistivity between 10^{-4} and $10^1 \text{ }\Omega\text{cm}$, depending on the deposition conditions [8]. Moreover, all these properties are achieved depositing the material at room temperature, which brings huge advantages, not only economically, but also concerning the enhanced range of applications that it brings, since it allows for the development of inexpensive transparent and flexible electronic circuits [1].

2. Experimental details

The devices were produced using $2.5 \times 2.5 \text{ cm}$ glass substrates coated with indium tin oxide and aluminum titanium oxide. The ITO and ATO layers were, respectively, the gate electrode and the gate insulator of the produced bottom-gate TFTs whose structure is schematically presented in figure 1.

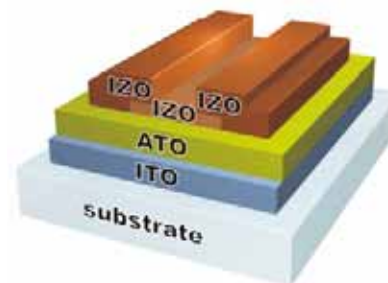


Figure 1. Schematic illustration of the IZO-based bottom-gate TFT structure. The width to length ratio (W/L) was 15.

The active layer and the source/drain electrodes were both based on IZO, deposited at room temperature by rf (13.56 MHz) magnetron sputtering, using a ceramic target from Super Conductor Materials, Inc. The power densities were 5 and 9 W/cm^2 , the O_2/Ar flow ratios were 0.15 and 0.02 (for the active layer and the source/drain electrodes, respectively) and the deposition pressure was 0.15 Pa. The patterning of the source/drain electrodes was performed by lift-

off, and the width-to-length ratio (W/L) used was 15, with L being 100 μm . The films thicknesses were measured by a surface profilometer Sloan Tech Dektak 3.

Concerning the electrical characterization, it was used an Alessi microprobe station and a semiconductor parameter analyzer Agilent 4155C, controlled by the software Metrics ICS. The characterization was performed using large delay times (4 seconds) between each data point, in order to minimize the parasitic effects of the measuring system. All the electrical characterization was performed in the dark, at room temperature, and a previously defined fitting procedure was used to extract the electrical parameters of all the obtained plots, in order to avoid errors related with the fitting range.

3. Results and discussion

Figure 2 shows the X-ray diffraction pattern for the amorphous IZO film used at the channel layer, deposited on corning 1737 glass substrate. An amorphous like behaviour is observed which was also confirmed by the corresponding electron diffraction pattern of the same film, shown at the inset. The same was also observed for the IZO film used at the drain/source regions, with lower resistivity. AFM analysis was also performed and the surface roughness of the films is very low being 2 nm for the IZO film used at the channel layer and 1.6 nm for the IZO film used at the source/drain regions.

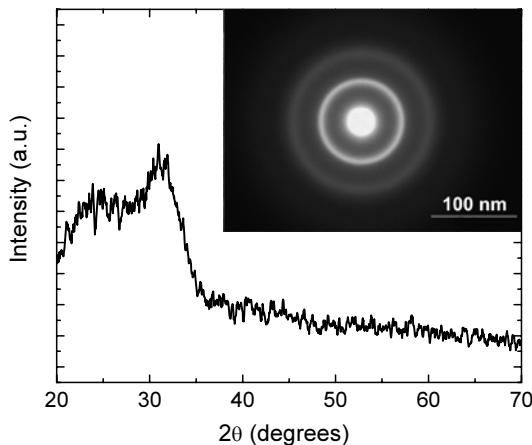


Figure 2. Typical X-ray diffractogram of an amorphous IZO film 200 nm produced by rf magnetron sputtering at room temperature with a partial oxygen pressure of 1.5×10^{-2} Pa, and used at the channel layer. The insets show the corresponding electron diffraction pattern of the same film.

In order to select the amorphous IZO films with the adequate electrical properties to be used as the active channel layer or at the source/drain TTFT regions, it was performed a study that consisted in varying the amount of oxygen present during the films deposition and to correlate it to the electrical properties by keeping the optical properties unaffected. Figure 3 shows the dependence of the electrical resistivity and the optical gap on the oxygen partial pressure used (PO_2). It was observed that as PO_2 increases the resistivity also increases. The highest resistivity ($\approx 10 \Omega\text{cm}$) was obtained for $\text{PO}_2 \approx 10^{-1}$ Pa, for the set of PO_2 used in this study. For this amount of oxygen the films became closer to stoichiometry and consequently higher resistive. As we decrease PO_2 , a deviation from stoichiometry is obtained accompanied by a decrease on the electrical resistivity, due to a lower carrier concentration or/and electron mobility. For the films with lower resistivity and used at the source/drain regions ($\approx 10^{-4} \Omega\text{cm}$), we measured Hall mobilities of about $60 \text{ cm}^2/\text{Vs}$ and an electron carrier concentration of $\approx 10^{19} \text{ cm}^{-3}$. The films produced are also optically transparent in the entire visible and near-infrared regions. The average optical transmittance is greater than 80%, including the reflection associated with the film and glass substrate. From this data and through the Tauc's plot (the imaginary part of the dielectric function near the band edge is taken assuming parabolic bands and a constant momentum matrix element), we inferred the optical gap.

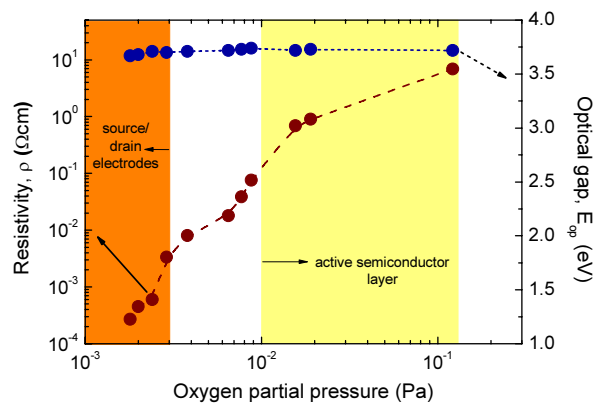


Figure 3. Dependence of the resistivity and the optical gap of amorphous IZO films on the oxygen partial pressure. The films have been deposited on 1 mm thick corning 1737 glass substrates.

The data reveal that for the range of PO_2 used the optical gap is almost constant to a value of 3.7 eV. These values are quite close to the ones observed on crystalline/polycrystalline IZO films (3.7-3.9 eV) [9].

Figure 4 shows the output and transfer characteristics obtained for a typical produced TTFTs. The output characteristics (here presented for the TTFT with 60 nm thick active layer) evidence high on-current, above 2.5 mA, a nice pinch-off and hard saturation, which is quite desirable for practical applications of the transistors [2, 10]. All the TTFTs are n-type and work in enhancement mode (i.e., threshold voltage, $V_T > 0$).

As it is observed the device present a low gate leakage current, of the order 10^{-10} A (several orders of magnitude lower than the source-to-drain current, which guarantees that the TTFT characteristics are unaffected by the gate leak current) for V_G values between -10 V to 20 V. The threshold gate voltage (V_T) was determined from the interception with V_G axis of the slope of the plot of versus V_G . We have obtained a $V_T = 2.5$ V, showing that the TTFT operates clearly in the enhancement mode. From the transfer characteristics it was also possible to calculate the channel mobility (obtained by the transconductance in the linear regime). The obtained value was $25 \text{ cm}^2/\text{Vs}$, exceeding the values reported by other TTFTs based in amorphous/polycrystalline oxide semiconductors, and two orders of magnitude higher than those obtained in conventional a-Si:H TFTs.

Figure 2b) shows a typical output source-to-drain current (I_D) - voltage (V_D) characteristics of the IZO TTFT, as a function of gate voltage. For $V_G = 0$ V the TTFT is off, and the current I_D markedly increases as V_D increases at a positive gate bias (V_G), indicating that the channel is n-type and the TTFT operates in the enhancement mode with the accumulation of electrons. The I_D reaches values up to about 2.5 mA, at $V_G = 20$ V. The I_D - V_D output characteristics exhibit a clear pinch-off voltage and a hard saturation current.

4. Conclusions

From the study performed we clear identify the new application of an amorphous IZO oxide as a viable active semiconducting material where the carrier's transport is due to preferential channel

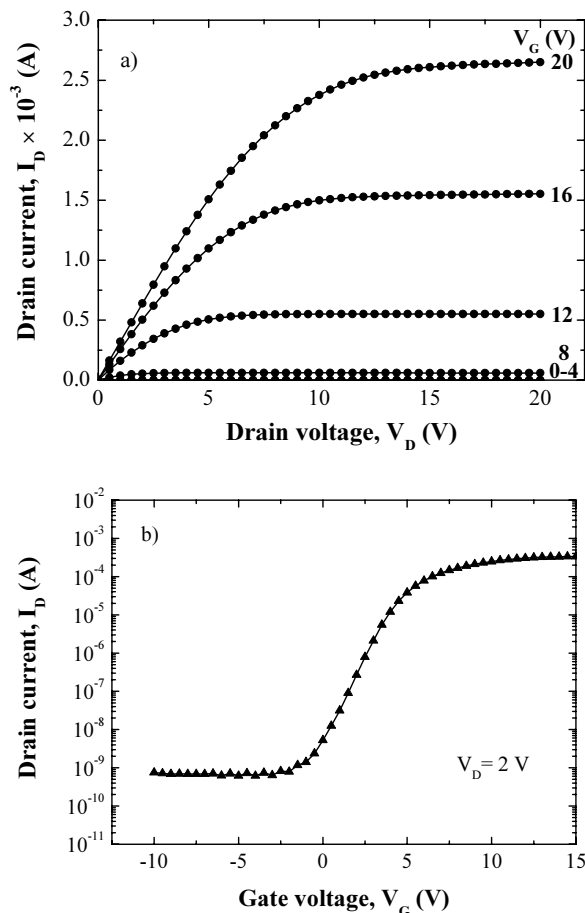


Figure 4. Output (a) and transfer (b) characteristics of the produced TTFTs with an active layer's thickness of 60 nm.

path formed by the direct overlap among the neighbouring s-like metal orbitals, reinforced by the presence of Zn atoms in the indium oxide matrix that make it insensitive to distorted metal-oxygen-metal chemical bonds that exist in the amorphous materials.

Therefore, we could produce fully amorphous or nanostructured IZO films that exhibit carriers' mobility similar to the one of crystalline counterparts. So, this material can be fully used for the fabrication of TTFT with excellent electrical performances, allowing its use not only as switching key but also in the drivers' conception, besides meeting the processing requirements for the new generation of low cost transparent and flexible electronics (deposition at room temperature and possible to be used over large areas). Furthermore, the technology used can be easily incorporated and it is compatible with others existing technologies to process large area displays. This will allow a fast mass production

integration of these TFTs for a wide ranging of applications where the first one will be active matrices for addressing displays, surpassing so the actual use of a-Si:H. Besides this, its incorporation with other p-type oxide semiconductors will open the field of other applications, such as CMOS like devices for digital electronics.

In other words “The future belongs to those who believe in the beauty of their dreams” (Eleanor Roosevelt).

4. Acknowledgements

The authors would like to express their thanks to the financial support given by the Portuguese Science Foundation (FCT-MCTES) during the last years. Part of this work is financed by SAIT (Samsung Advanced Institute of Technology), South Korea. The authors thank Planar Systems, Inc., Espoo, Finland, for supplying the ITO/ATO glass substrates.

5. References

- [1] E. Fortunato, P. Barquinha, A. Pimentel, A. Gonçalves, A. Marques, L. Pereira, R. Martins, *Adv. Mater.* 17, 590 (2005).
- [2] R.L. Hoffman, B.J. Norris, J.F. Wager, *Appl. Phys. Lett.* 82, 733 (2003).
- [3] P.F. Carcia, R.S. McLean, M.H. Reilly, G. Nunes, *Appl. Phys. Lett.* 82, 1117 (2003).
- [4] B.J. Norris, J. Anderson, J.F. Wager, D.A. Keszler, *J. Phys. D: Appl. Phys.* 36, L105 (2003).
- [5] K. Nomura, H. Ohta, A. Takagi, T. Kamiya, M. Hirano, H. Hosono, *Nature* 432, 488 (2004).
- [6] H.Q. Chiang, J.F. Wager, R.L. Hoffman, J. Jeong, D.A. Keszler, *Appl. Phys Lett.* 86, 1 (2005).
- [7] N.L. Dehuff, E.S. Kettenring, D. Hong, H.Q. Chiang, J.F. Wager, R.L. Hoffman, C.-H. Park, D.A. Keszler, *J. Appl. Phys.* 97, 1 (2005).
- [8] R. Martins, P. Barquinha, A. Pimentel, L. Pereira, E. Fortunato, *phys. stat. sol. (a)* 202, No.9, R95-R97 (2005).
- [9] a) T. Minami, T. Kakumu, Y. Takeda, S. Takata, *Thin Solid Films* 290-291, 1 (1996),
b) N. Naghavi, C. Marcel, L. Dupont, A.

Rougier, J.B. Leriche, C. Guéry, J. Mater. Chem. 10, 2315 (2000), c) T. Sasabayashi, N. Ito, E. Nishimura, M. Kon, P.K. Song, K. Utsumi, A. Kaijo, Y. Shigesato, *Thin Solid Films* 445, 219 (2003).

- [10] E. Fortunato, P. Barquinha, A. Pimentel, A. Gonçalves, A. Marques, R. Martins, L. Pereira, *Appl. Phys. Lett.* 85 2541 (2004).